*Russian Geology and Geophysics* © 2019, V.S. Sobolev IGM, Siberian Branch of the RAS
*Vol. 60, No. 1, pp. 33–44, 2019* *DOI:10.15372/RGG2019003* *Geologiya i Geofizika*

# $^{40}Ar/^{39}Ar$ Geochronology of Alkaline Rocks of the Inagli Massif (Aldan Shield, southern Yakutia)

**A.V. Ponomarchuk [a,✉], I.R. Prokop'ev [a,b], T.V. Svetlitskaya [a], A.G. Doroshkevich [a,c]**

[a] *V.S. Sobolev Institute of Geology and Mineralogy, Siberian Branch of the Russian Academy of Sciences, pr. Akademika Koptyuga 3, Novosibirsk, 630090, Russia*
[b] *Novosibirsk State University, ul. Pirogova 2, Novosibirsk, 630090, Russia*
[c] *Institute of Geology, Siberian Branch of the Russian Academy of Sciences, ul. Sakh'yanovoi 6a, Ulan-Ude, 670047, Russia*

Received 22 June 2017; received in revised form 27 February 2018; accepted 15 June 2018

**Abstract—**The Inagli zoned ring massif is located in the Central Aldan ore district. The close localization of ultrabasic and alkaline potassic rocks, magmatism, and mineralization (platinum, gems Cr-diopside, and vermiculite) make this object unique from both geological and economic perspectives. Formation of alkaline rocks in the Inagli massif was related to the Mesozoic tectonomagmatic activation of the Aldan Shield and occurred in several stages. Intrusion of clinopyroxenites took place no later than 145.8 ± 3.2 Ma, whereas most of alkaline rocks of the ring framing formed at 133–128 Ma. The feldspar-Cr-diopside-mica veins in the dunite core are dated at 133.4 ± 1 Ma.

*Keywords:* Inagli massif, Ar–Ar dating, zoned ring massifs, dating of alkaline rocks, Mesozoic igneous rocks

## INTRODUCTION

Investigation of zoned ring alkaline-ultrabasic massifs of the Aldan Shield has been going on for over 50 years, however, the time and formation mechanisms of these intrusions have still not been agreed upon. The Konder and Inagli massifs are characterized by platinum mineralization different from those in the stratified intrusions of the Bushveld complex (the South African Republic) (Campbell et al., 1983; Cawthorn et al., 2002), the dunites of Nizhnii Tagil (Malich, 1999; Genkin, 1997) in the Urals region, and other sites. Aside from that, the studied Inagli massif has a unique deposit of gems Cr-diopside (Yakutian "emerald") and vermiculite, whose formation was associated with metasomatic processes and recrystallization within the alkaline-ultramafic complex.

Geochronology (El'yanov and Moralev, 1961; Kostyuk et al., 1990; Pushkarev et al., 2002; Malitch et al., 2012; Shukolyukov et al., 2012; Ronkin et al., 2013), paleomagnetic research (Ugryumov and Kiselev, 1969; Karetnikov, 2009), and geological observations (Shnai et al., 1980; Kostyuk et al., 1990; Okrugin, 2004) do not provide conclusive data on the time and formation stages of the alkaline and ultrabasic rocks of the Konder and Inagli massifs. Among the two, the alkaline-ultramafic Konder massif in the Khabarovsk Krai is better studied in terms of geochronology. According to the previous studies, the massif's formation occurred at least in two magmatic stages, namely the early Proterozoic associated with ultramafic melt intrusion, and the overlapping late Mesozoic with the formation of kosvites, monzonite-type elements, and other alkaline rocks (Gurovich et al., 1994; Karetnikov, 2009; etc.). However, multiple K–Ar dating efforts are found in the literature (El'yanov and Moralev, 1961; Kostyuk et al., 1990; Maksimov et al., 2010; etc.), which confirm the Mesozoic age of both the dunite core and the outer intrusion ring of the Konder and Inagli massifs. Age estimates of the ultrabasic and alkaline rocks range between 150 and 100 Ma, with estimates under 80 Ma also available, and therefore the accuracy and reliability of these results require further study.

The Inagli massif is located in the Central Aldan ore district (Vetluzhskikh, 1990), a major industrial district of southern Yakutia (Fig. 1) and also a major area of Mesozoic alkaline rocks and gold mineralization associated with them (Vetluzhskikh, 1990; Vetluzhskikh et al., 2002; Maksimov, 2003; Kochetkov, 2006). Although, alkaline rocks are closely associated with alkaline-ultrabasic and ultramafic rocks in a number of massifs (for instance, the Yakokut and Ryabinovyi massifs), they are still much less common there, then in the Inagli massif. Thus, the correlation between the formation stages of the Inagli massif and other massifs of the Central Aldan district and the Aldan Shield in general by time and genesis becomes a crucial aspect. The genesis of these massifs is inextricably tied to the data on their formation age. The current concepts may be reduced to the two following models:

(1) the massifs originated from the homogeneous original melt in the course of crystallization-gravitational differentiation in the Mesozoic (Kostyuk et al., 1990; Okrugin, 2004);

✉ Corresponding author.
*E-mail adress:* antponomar@gmail.com (A.P. Ponomarchuk)

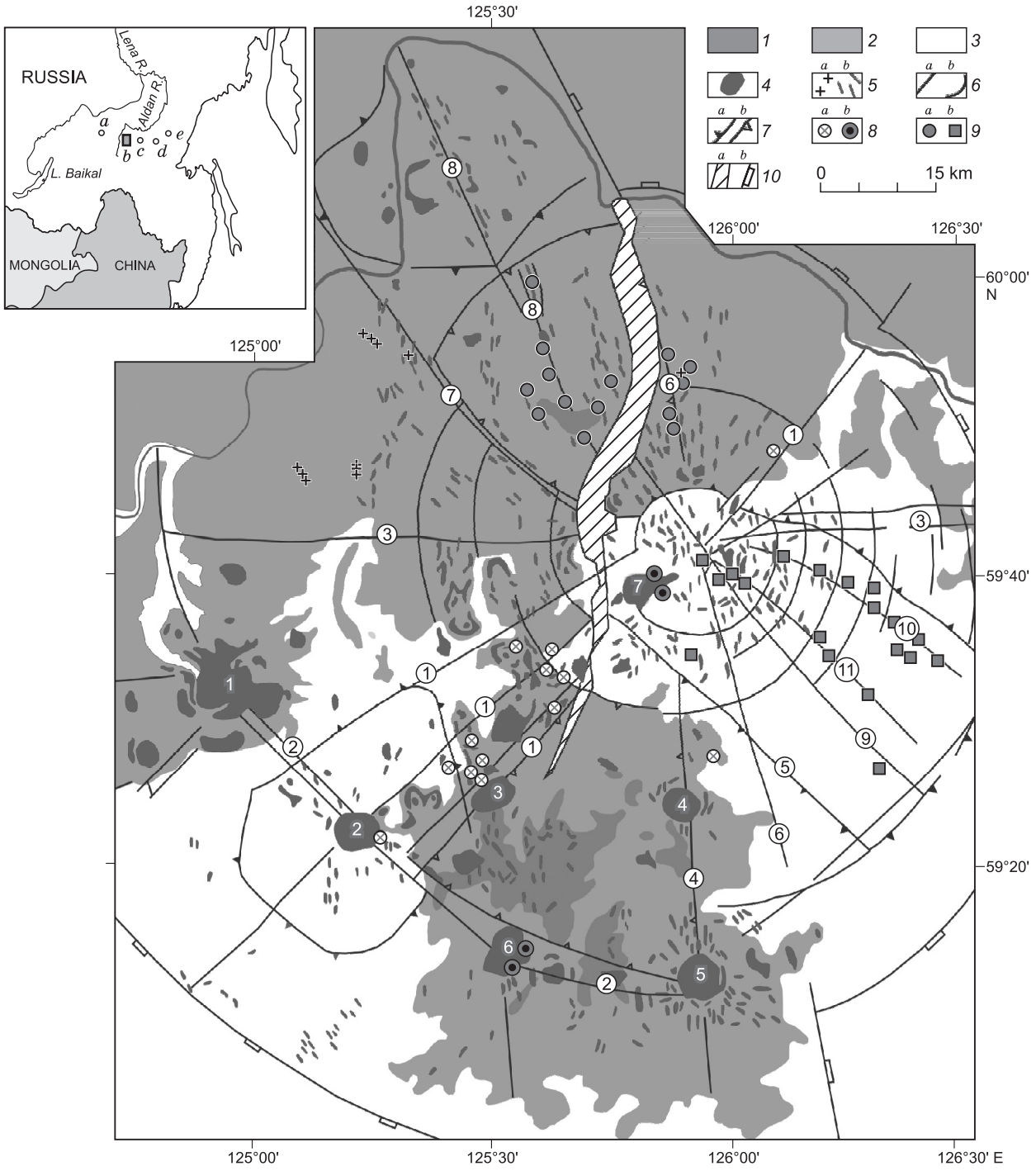


**Fig. 1.** Geological structure scheme of the Central Aldan ore district (modified from (Maksimov et al., 2010)). *1*, Upper and Middle Jurassic terrigenous deposits; *2*, Vendian–lower Cambrian platform cover; *3*, early Cambrian crystalline basement; *4–5*, alkaline and moderately alkaline magmatic manifestations: intrusions (*4*), diatremes (*5a*), and dikes (*5b*); *6*, faults: proven (*a*), predicted (*b*); *7*, outlines of structural blocks: uplifts (*7a*), troughs (*7b*); *8–9*, deposits of formations: sulfide gold (*8a*), porphyry gold (*8b*), gold–argillisite–K-feldspar–quartz (*9a*), gold–molybdenite–brannerite–gumbaite (*9b*); *10a*, Yakokut valley graben, *10b*, outer interface of the Central Aldan ore-magmatic system (CAOMS). Major intrusive massifs: 1, Inagli, 2, Tommot, 3, Yakokut, 4, Dzhekonda, 5, Yllymakh, 6, Yukhta, 7, Ryabinovyi. The insert shows locations of massifs and ore districts: *a*, Malyi Murun massif; *b*, Central Aldan ore district; *c*, Dzheltula massif; *d*, Ket-Kap–Yuna district; *e*, Konder massif.

(2) the massifs are polychronic and heterogeneous, as they combine formations of dunites alkaline gabbro rims, pyroxenites, as well as alkaline and subalkaline acid rocks. Here, the dunite core is considered as either Precambrian (El'yanov and Moralev, 1961) or Mesozoic (Maksimov et al., 2010).

New data on Ar–Ar dating of alkaline rocks of the ring and secondary changes imposed on the core of the Inagli massif are provided in the present paper. The results obtained provide a reliable chronology of rock intrusions and transformations as well.

## BRIEF GEOLOGICAL CHARACTERISTICS OF THE INAGLI MASSIF

The Inagli massif of ultrabasic and alkaline rocks is located in the northwest of the Central block of Aldan Shield (Sakha Republic (Yakutia)) 30 km to the west of the city of Aldan (Fig. 1). It is a pipe-shaped body, which appears round in plain view, with an area of about 20 km$^2$ (Fig. 2) located at the intersection of two regional fault systems—Yukhta and Inagli—with northwestern and northeastern strike, respectively (Okrugin, 2004). The geological structure of the Inagli massif is described in a number of papers (Bilibin, 1958; Rozhkov et al., 1962; Korchagin, 1966; Glagolev et al., 1974; Maksimov, 1975; Kochetkov, 1984; Kostyuk et al., 1990). The massif has a zoned ring structure. Its core (the area of about 16 km$^2$) is composed of a dunite layer with a thickness of about 1 km based on the well data and over 5 km based on geophysical surveys. Dunites at the periphery are surrounded by olivine- and phlogopite-containing clinopyroxenites, melanocratic pyroxenic syenites, and shonkinites with counter veins of Mesozoic alkaline syenite-pegmatites. Dunite xenoliths are observed in shonkinites (Fig. 3*b*). Apart from the northwestern part, the Inagli massif is rimmed with post-Jurassic bed-like syenite-monzonite porphyry intrusions. Pegmatite veins (Cr-diopside-orthoclase, orthoclase-amphibole, and microcline-albite-amphibole with aegirine) fill ring and radial fractures in the inner part and at the periphery of the dunite core of the massif and partially intrude into the alkaline rock development area. The central part of the Inagli massif formed by dunites was eroded, thereby forming a depression that lies at the base of the Inagli platinum placer deposit.

The host rocks of the massif have a two-stage structure. The lower stage is formed by Archean strongly dislocated crystalline schists, gneisses, and amphibolites breached by Archean alaskite granites. The upper stage is fragmentary and represented by late Proterozoic sandstones and gritstones, limestones, and lower Cambrian dolomites. Tectonic contacts between the massif and its host rocks are vertical or steeply dipping. No direct contact between dunites and gritstones at the base of the Proterozoic mass are discovered,

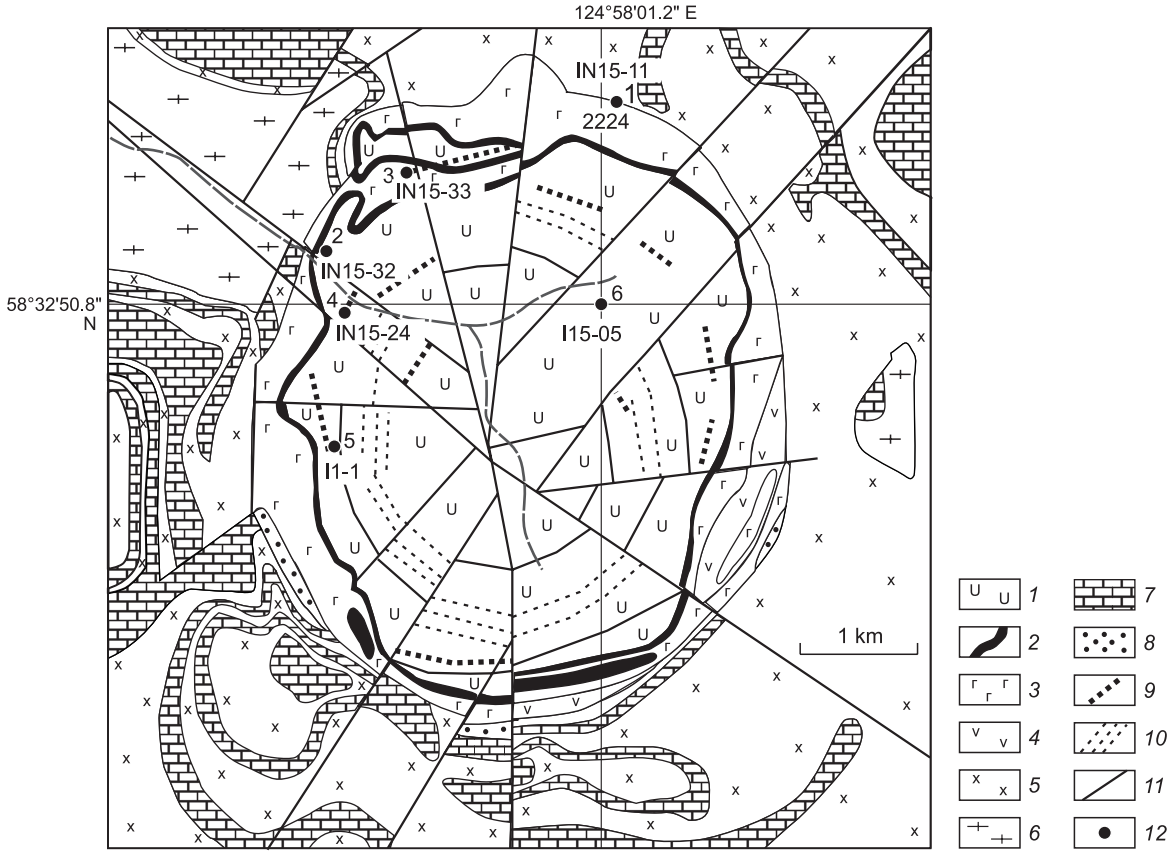


**Fig. 2.** Geological structure scheme of the Inagli massif (modified from (Glagolev et al., 1974)) with sampling sites for geochronological studies. *1*, dunites; *2*, pyroxenites; *3*, shonkinites; *4*, leucocratic syenites; *5*, monzonite porphyry; *6*, Fedorov series rocks; *7*, carbonate rocks; *8*, gritstones and sandstones; *9*, syenite and pegmatite dikes; *10*, ring fractures with metasomatites; *11*, faults; *12*, sampling sites and sample numbers.

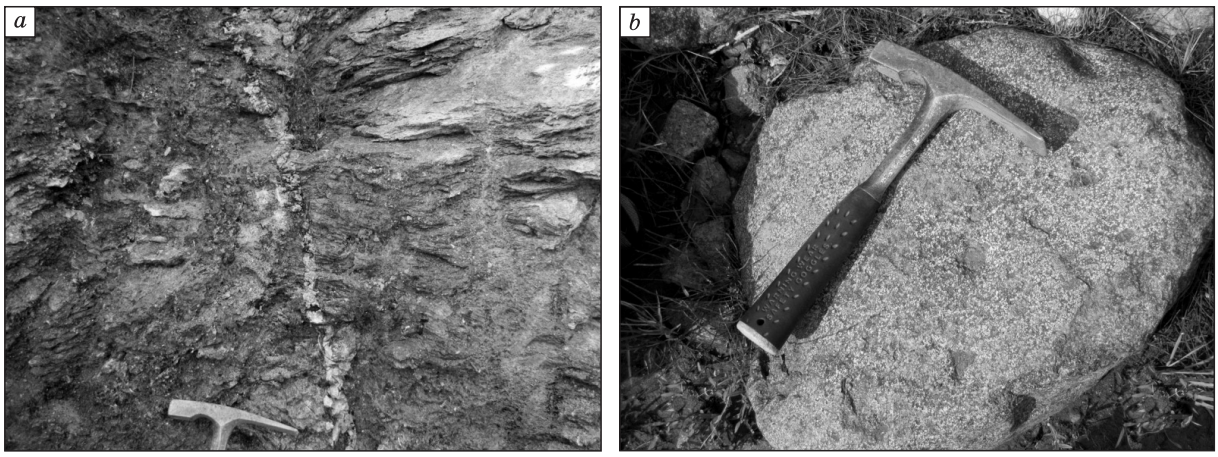


**Fig. 3.** Images of Inagli massif rocks demonstrating relationships between various rocks. *a*, Late syenite counter vein in a chrome diopside body; *b*, dunite xenoliths in shonkinites.

however sharp contacts with shonkinites-syenite porphyry are observed. Proterozoic and Cambrian gritstones and sandstones show various degrees of metamorphism with fragments transformed into biotite-quartzite gneisses.

According to the earlier papers, dunites are consertal and have a panidiomorphic structure in weakly serpentinized differences and cellular structure in the strongly serpentinized ones. They consist of olivine (40–85%), serpentine (15–60%), chrome spinel (up to 3%), magnetite (up to 3%), Cr-diopside (up to 3%), and phlogopite (up to 3%) (Korchagin, 1966; Mues-Schumacher et al., 1996). The contact area of dunites and shonkinites has a narrow (about 50 m) olivine-clinopyroxenic rim with mica (peridotites according to (Korchagin, 1966; Ugryumov and Kiselev, 1969)). The mineral composition of the rocks changes from phlogopite- and K-feldspar-containing olivine clinopyroxenites at the interface with dunites to apatite-containing olivine-free phlogopite clinopyroxenites at the interface with shonkinites. Olivine-clinopyroxenic rocks from the middle part of the rim include 45–50% clinopyroxene, 35–40% olivine, up to 10% serpentine, up to 5% K-feldspar, 2–3% phlogopite, and 2–3% apatite. A narrow zone of strongly serpentinized dunites with high platy magnetite content is observed between these rocks and dunites, whereas the transition into shonkintes is characterized as gradual (Korchagin, 1996). Shonkinites and melanocratic pyroxenic syenites consist of clinopyroxene (20–45%), K-feldspar (20–65%), phlogopite (1–25%), apatite (1–7%), and magnetite (1–5%), while olivine- and/or pseudoleucite-containing differences also include olivine (up to 15%) and/or pseudoleucite (up to 10%), respectively.

A zone of stockwork veins and pockets of feldspar-chrome diopside-mica giant-grained rocks is identified in the southwest of the dunite core, to which the Inagli Cr-diopside deposit is confined. According to (Korchagin, 1966), these ore-bearing bodies with thicknesses from tens of centimeters to meters develop around diopside-orthoclasic and microcline-albite-amphibolic pegmatite counter veins in dunites and often include relict fragments of the latter. In addition, late amphibole-feldspar counter veins (with thicknesses of tens of centimeters) are found in Cr-diopside metasomatites in the quarry outcrop (Fig. 3*b*). These geological observations are indications of multistage processes that transform ultrabasic and alkaline rocks of the massif.

## ROCK PETROGRAPHY OF THE MASSIF

**Dunites** have a medium-grained structure. Olivine in the rocks is intensely serpentinized (up to 20% replacement). Primary chromite is transformed into chrome magnetite. Isolated phlogopite scales can be seen near ore grains. The petrographic data available do not make it possible to conclusively identify phlogopite in dunites as syngenetic or as a result of later metasomatic transformations (Fig. 4*a*).

**Phlogopite clinopyroxenites** are characterized by cumulative texture and hypidiomorphic medium to large-grained structure (Fig. 4*b*). Clinopyroxene content in the rocks reaches 60%. Interstitial phlogopite adds up to 30% of the rock volume. Clinopyroxenites also include up to 10% of apatites. The mineral forms large idiomorphic crystals and microinclusions in clinopyroxene and phlogopite. Ore mineral content in the rocks reaches 5%. Magnetite is crystallized both in the form of idiomorphic grains and interstitial xenomorphic formations. Isolated sulfide grains may be found in clinopyroxene.

Pegmatite amphibole-feldspar veins are giant-grained rocks consisting of orthoclase, microcline, and eckermannite.

**Shonkinites** and **syenites** are characterized by large- and medium-grained structure and massive or trachytoid texture. Shonkinites consist of clinopyroxene (30%), K-feldspar (30%), pseudoleucite (7–10%), phlogopite (15%), apatite (2–5%), olivine (10%), and titanium magnetite (1–5%) (Fig. 4*c*).

Syenites are formed by clinopyroxene (20%), K-feldspar (60%), phlogopite (7–10%), olivine (up to 5%), apatite (1–

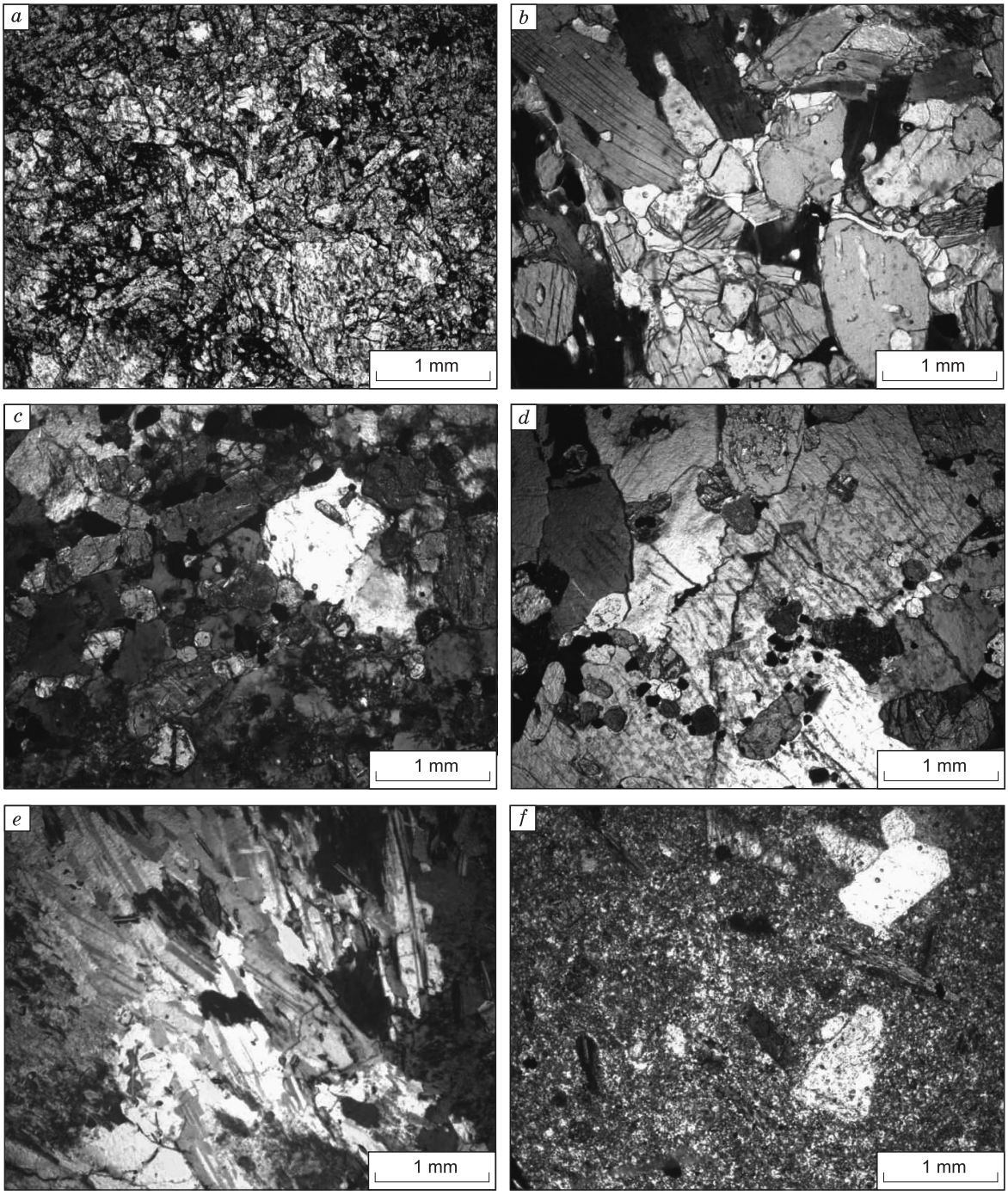


**Fig. 4.** Images of thin sections of the main types of Inagli massif rocks. *a*, Dunite with phlogopite impregnation (sample IN15-05, parallel nicols); *b*, phlogopite clinopyroxenite (sample IN-15-32, crossed nicols); *c*, shonkinite (sample 2224, crossed nicols); *d*, melanocratic syenite (sample IN-15-33, crossed nicols); *e*, leucocratic syenite (sample IN-15-24, crossed nicols); *f*, monzonite porphyry (sample IN-15-11, crossed nicols).

2%), and titanium magnetite (1–4 %) (Fig. 4*d*). Alkaline syenites consisting of K-feldspar (about 90%), aegirine, and richterite, an alkaline amphibole (up to 10%), may be found in the rocks of the massif (Fig. 4*e*). The rocks are often intensely albitized.

Phenocrysts in **monzonite porphyry** are represented by oblong-prismatic hornblende crystals (up to 0.5 cm), large (up to 1 cm) zonal plagioclase and K-feldspar phenocrysts (Fig. 4*f*), while the main body consists of quartz and K-feldspar. In general, the mineral composition of the rocks is as follows: plagioclase (up to 50%), hornblende (25%), K-feldspar (15%), quartz (8%), ore minerals (up to 2%, titanium magnetite and sulfides). The rocks also include zircon and apatite (less than 1%).

## FACTUAL RESEARCH DATA

To perform geochronological and isotopic research in surveying seasons 2012–2015, the alkaline rock mass and dunite core samples were collected. Sample sites and numbers are indicated on the geological scheme of the massif (Fig. 2).

**Measurement technique.** $^{40}Ar/^{39}Ar$ dating was performed using monomineral fractions collected manually under binocular magnifier from the loosened sample fraction sized 0.3–0.1 mm. The samples were irradiated in a cadmium-plated channel of the scientific-grade BBP-K reactor at the Scientific Research Institute of Nuclear Physics (Tomsk, Russia). Neutron flux gradient did not exceed 0.5% in the sample size during the irradiation period. MCA-11 muscovite, a standard K/Ar sample (industry standard reference material No. 129-88) prepared by the All-Soviet Scientific Research Institute of Mineral Raw Materials of the Ministry of Geology of the USSR in 1988 was used as a monitor. International standard Bern 4m muscovite and LP-6 biotite samples were used for the sample's calibration as a $^{40}Ar/^{39}Ar$ monitor (Baksi et al., 1996). Based on the calibration results, the average of 311.0 ± 1.5 Ma was accepted as the MCA-11 muscovite age (Travin, 2016). According to (Steiger and Jäger, 1977), total decay constant $^{40}K$ was assumed to be $5.543 \times 10^{-10}$ $yr^{-1}$.

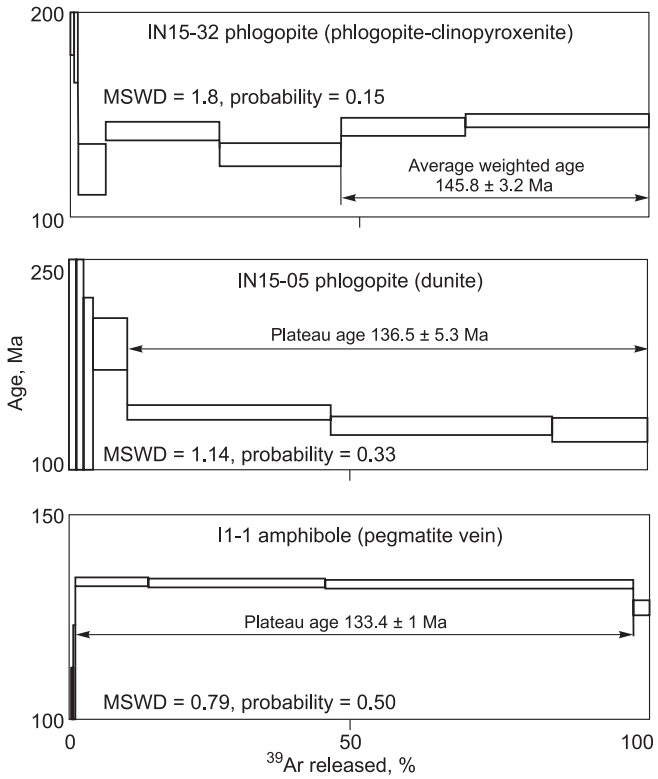


**Fig. 5.** $^{40}Ar/^{39}Ar$ dating results for monomineral phlogopite fractions from phlogopite clinopyroxenites (sample IN15-32), phlogopite phenocrysts in dunites (sample IN15-05), and amphibole from amphibole-feldspar veins (sample I1-1) in the Inagli massif. The error is presented with ±2σ interval.

A blank test to determine $^{40}Ar$ (10 min at 1200 °C) did not exceed $5 \times 10^{-10}$ ncm$^3$. Argon purification was performed using Ti- and ZrAl-SAES-getters. Additional purification was carried out using quartz appendage submerged into liquid nitrogen. The isotopic composition of argon was measured using the Noble gas 5400 mass spectrometer by Micromass (England). To make adjustments for $^{36}Ar$, $^{37}Ar$, and $^{40}Ar$ obtained in course of Ca and K irradiation, the following coefficients were used: $(^{39}Ar/^{37}Ar)_{Ca}$ = 0.000891 ± 0.000005, $(^{36}Ar/^{37}Ar)_{Ca}$ = 0.000446 ± 0.000006, $(^{40}Ar/^{39}Ar)_{K}$ = 0.089 ± 0.001. Special attention was paid to controlling the isotopic discrimination factor via measuring the portion of the purified atmospheric argon. Average $^{40}Ar/^{36}Ar$ relationship as of the measurement period was 295.5 ± 0.5. The sample was heated in the quartz reactor placed in the resistance furnace. Dating was carried out via gradual warm-up. The temperature was controlled using a chromel-alumel thermocouple. Temperature regulation accuracy was ±1 °C.

**Research results.** Based on the results of the $^{40}Ar/^{39}Ar$ geochronology study, a phlogopite clinopyroxenite age spectrum was obtained (sample IN15-32, Fig. 2, Table 1). It consists of seven stages (Fig. 5). The age spectrum obtained shows signs of argon loss and does not make it possible to identify the age plateau (Fleck et al., 1977). In this case, the value closest to the factual sample age is identified by the weighted average of the two last stages, i.e., 145.8 ± 3.2 Ma. The amount of gas released in the two last stages is 55%.

The $^{40}Ar/^{39}Ar$ spectrum for phlogopite from dunites (sample IN15-05, Fig. 2, Table 2) consists of seven stages (Fig. 5). The last three stages satisfy the age plateau criterion and define the average weighted age of the studied sample at 136.5 ± 5.3 Ma. The amount of $^{39}Ar$ released within the age plateau equals 90% of the total $^{39}Ar$ volume released from the sample in course of the experiment.

Pegmatite amphibole-feldspar veins breaching the dunite core (sample I1-1, Fig. 2, Table 1) were dated based on amphibole. The amphibole age spectrum consists of six stages, with the age plateau formed by the last four stages with 95% of $^{39}Ar$ released, which defines a narrow mineral formation period of 133.4 ± 1 Ma (Fig. 5, Table 1) and fits with vein formation time.

The $^{40}Ar/^{39}Ar$ age spectrum for phlogopite from melanocratic syenite (sample IN15-33, Fig. 2, Table 1) consists of 8 stages (Fig. 6). The last four stages for the plateau with 80% of $^{39}Ar$ released. According to the plateau, the average weighted phlogopite formation age is 133.2 ± 2.2 Ma (Table 1), which may be accepted as the melanocratic syenite formation time.

Amphibole from leucocratic syenites (sample IN15-24, Fig. 2, Table 1) demonstrates a disturbed age spectrum. The latter consists of six stages (Fig. 6) with the pseudoplateau defined based on three stages, which identifies the average weighted age of 113.3 ± 3.4 Ma (Fig. 6), along with a large high-temperature stage of 128.2 ± 4.4 Ma (Table 1). Three stages forming the pseudo-plateau account for 40% of $^{39}Ar$

**Table 1.** Ar–Ar dating results for Inagli massif rocks

| *T*, °C | $^{40}Ar/^{39}Ar$ | ±2σ | $^{38}Ar/^{39}Ar$ | ±2σ | $^{37}Ar/^{39}Ar$ | ±2σ | $^{36}Ar/^{39}Ar$ | ±2σ | Released $^{39}Ar$, % | Age, Ma | ±2σ |
|---|---|---|---|---|---|---|---|---|---|---|---|
| IN15-32 phlogopite (Integral age 142.3 ± 2.5 Ma; J = 0.003970 ± 0.000041) | | | | | | | | | | | |
| 500 | 109.5 | 2.4 | 0.11 | 0.08 | 0.21 | 0.07 | 0.24 | 0.02 | 0.6 | 265.1 | 39.9 |
| 620 | 92.8 | 3.1 | 0.07 | 0.03 | 0.7 | 0.2 | 0.17 | 0.03 | 1.3 | 281.7 | 62.1 |
| 750 | 37.7 | 0.2 | 0.026 | 0.007 | 0.09 | 0.01 | 0.067 | 0.006 | 6.1 | 123.4 | 12.5 |
| 860 | 25.44 | 0.06 | 0.020 | 0.002 | 0.021 | 0.005 | 0.016 | 0.002 | 25.8 | 142.1 | 4.6 |
| 960 | 24.24 | 0.06 | 0.018 | 0.003 | 0.004 | 0.003 | 0.019 | 0.003 | 46.8 | 128.6 | 5.2 |
| 1050 | 24.96 | 0.05 | 0.015 | 0.001 | 0.033 | 0.002 | 0.014 | 0.002 | 68.3 | 144.1 | 4.4 |
| 1140 | 24.88 | 0.04 | 0.015 | 0.002 | 0.018 | 0.006 | 0.012 | 0.001 | 100.0 | 147.2 | 3.2 |
| IN15-05 phlogopite (Integral age 138.7 ± 4.8 Ma; J = 0.003984 ± 0.000042) | | | | | | | | | | | |
| 550 | 1003.7 | 65.6 | 0.55 | 0.09 | 10.5 | 2.7 | 3.3 | 0.2 | 1.3 | 167.4 | 126.9 |
| 680 | 240.0 | 12.2 | 0.15 | 0.03 | 10.5 | 3.3 | 0.75 | 0.06 | 4.1 | 123.2 | 100.6 |
| 830 | 81.6 | 0.8 | 0.05 | 0.02 | 3.7 | 3.0 | 0.182 | 0.010 | 10.0 | 190.3 | 18.5 |
| 980 | 27.41 | 0.07 | 0.026 | 0.003 | 0.3 | 0.2 | 0.023 | 0.003 | 45.2 | 141.6 | 5.3 |
| 1080 | 21.82 | 0.07 | 0.014 | 0.003 | 0.2 | 0.2 | 0.009 | 0.003 | 83.5 | 132.2 | 6.6 |
| 1180 | 24.8 | 0.1 | 0.018 | 0.004 | 1.3 | 0.8 | 0.021 | 0.005 | 100.0 | 128.7 | 9.7 |
| I1-1 amphibole (Integral age 132.7 ± 1 Ma; J = 0.002892 ± 0.000022) | | | | | | | | | | | |
| 550 | 155.9 | 2.4 | 0.09 | 0.02 | 0.008 | 0.008 | 0.48 | 0.02 | 0.3 | 71.4 | 23.3 |
| 650 | 55.4 | 0.7 | 0.02 | 0.01 | 0.007 | 0.007 | 0.12 | 0.01 | 0.7 | 94.1 | 18.5 |
| 800 | 127.5 | 1.4 | 0.07 | 0.01 | 0.11 | 0.09 | 0.36 | 0.01 | 1.1 | 106.6 | 16.5 |
| 925 | 31.05 | 0.01 | 0.0170 | 0.0003 | 0.542 | 0.003 | 0.0151 | 0.0004 | 13.6 | 133.7 | 1.1 |
| 1000 | 29.07 | 0.01 | 0.0158 | 0.0001 | 0.565 | 0.001 | 0.0086 | 0.0002 | 44.2 | 133.4 | 1.0 |
| 1065 | 27.747 | 0.01 | 0.01499 | 0.0001 | 0.5846 | 0.001 | 0.0043 | 0.0002 | 97.5 | 133.2 | 1.0 |
| 1130 | 30.30 | 0.03 | 0.019 | 0.001 | 0.57 | 0.01 | 0.017 | 0.001 | 100.0 | 127.3 | 1.8 |
| IN15-33 phlogopite (Integral age 127.9 ± 2 Ma; J = 0.003999 ± 0.000042) | | | | | | | | | | | |
| 500 | 43.2 | 0.8 | 0.07 | 0.02 | 4.1 | 0.5 | 0.14 | 0.02 | 1.4 | 23.3 | 36.9 |
| 620 | 27.6 | 0.4 | 0.03 | 0.01 | 1.2 | 1.1 | 0.06 | 0.01 | 4.3 | 66.2 | 27.8 |
| 740 | 23.33 | 0.05 | 0.023 | 0.003 | 0.3 | 0.2 | 0.021 | 0.002 | 12.2 | 119.9 | 4.2 |
| 850 | 24.28 | 0.09 | 0.013 | 0.006 | 0.8 | 0.2 | 0.024 | 0.004 | 18.7 | 119.6 | 7.1 |
| 970 | 22.01 | 0.04 | 0.0177 | 0.0008 | 0.2 | 0.1 | 0.010 | 0.002 | 42.3 | 132.4 | 3.4 |
| 1060 | 23.21 | 0.06 | 0.021 | 0.003 | 0.4 | 0.2 | 0.010 | 0.003 | 52.1 | 140.2 | 5.5 |
| 1130 | 20.63 | 0.02 | 0.019 | 0.001 | 0.13 | 0.02 | 0.0058 | 0.0009 | 87.4 | 131.7 | 2.2 |
| 1170 | 21.88 | 0.03 | 0.018 | 0.001 | 0.14 | 0.04 | 0.009 | 0.001 | 100.0 | 134.4 | 2.7 |
| IN15-24 amphibole (Integral age 122.2 ± 3.7 Ma; J = 0.00004092 ± 0.000044) | | | | | | | | | | | |
| 550 | 134.4 | 8.8 | 0.14 | 0.07 | 12.6 | 5.7 | 0.36 | 0.07 | 1.3 | 190.1 | 129.2 |
| 700 | 30.7 | 0.2 | 0.015 | 0.006 | 0.5 | 0.3 | 0.044 | 0.008 | 8.9 | 125.8 | 16.5 |
| 850 | 27.3 | 0.2 | 0.021 | 0.007 | 2.3 | 0.7 | 0.040 | 0.008 | 18.9 | 110.8 | 15.8 |
| 970 | 31.5 | 0.1 | 0.02 | 0.01 | 0.9 | 0.5 | 0.055 | 0.003 | 27.1 | 109.0 | 7.2 |
| 1080 | 23.48 | 0.04 | 0.020 | 0.004 | 0.5 | 0.2 | 0.025 | 0.002 | 51.0 | 114.3 | 3.4 |
| 1170 | 21.84 | 0.05 | 0.022 | 0.001 | 0.5 | 0.1 | 0.013 | 0.002 | 100.0 | 128.2 | 4.4 |
| IN15-11 ground mass (Integral age 132 ± 2.2 Ma; J = 0.003953 ± 0.000041) | | | | | | | | | | | |
| 500 | 185.8 | 17.9 | 0.6 | 0.2 | 1.3 | 0.3 | 0.5 | 0.1 | 0.3 | 223.1 | 178.4 |
| 650 | 28.8 | 0.3 | 0.018 | 0.008 | 0.14 | 0.04 | 0.04 | 0.01 | 4.7 | 119.4 | 19.7 |
| 780 | 23.01 | 0.03 | 0.018 | 0.005 | 0.11 | 0.01 | 0.014 | 0.001 | 18.0 | 128.3 | 2.7 |
| 880 | 21.44 | 0.05 | 0.015 | 0.002 | 0.094 | 0.005 | 0.007 | 0.002 | 41.0 | 130.9 | 4.4 |
| 980 | 20.78 | 0.02 | 0.0188 | 0.0008 | 0.042 | 0.003 | 0.005 | 0.001 | 77.6 | 131.2 | 2.4 |
| 1065 | 23.36 | 0.01 | 0.0189 | 0.0008 | 0.073 | 0.005 | 0.009 | 0.001 | 90.4 | 139.9 | 1.7 |
| 1140 | 23.59 | 0.08 | 0.025 | 0.003 | 0.130 | 0.010 | 0.012 | 0.003 | 100.0 | 135.8 | 6.4 |

(*continued on next page*)

Table 1 (*continued*)

| *T*, °C | $^{40}Ar/^{39}Ar$ | ±2σ | $^{38}Ar/^{39}Ar$ | ±2σ | $^{37}Ar/^{39}Ar$ | ±2σ | $^{36}Ar/^{39}Ar$ | ±2σ | Released $^{39}Ar$, % | Age, Ma | ±2σ |
|---|---|---|---|---|---|---|---|---|---|---|---|
| 2224 phlogopite (Integral age 128.2 ± 2.6 Ma; J = 0.003572 ± 0.000033) | | | | | | | | | | | |
| 500 | 108.7 | 6.2 | 0.07 | 0.05 | 0.3 | 0.2 | 0.27 | 0.06 | 0.8 | 175.9 | 99.6 |
| 650 | 41.2 | 0.6 | 0.05 | 0.02 | 0.07 | 0.04 | 0.05 | 0.01 | 3.6 | 169.0 | 23.7 |
| 800 | 29.6 | 0.2 | 0.03 | 0.01 | 0.02 | 0.02 | 0.018 | 0.006 | 11.1 | 149.3 | 11.3 |
| 930 | 27.98 | 0.09 | 0.014 | 0.005 | 0.02 | 0.01 | 0.032 | 0.003 | 23.1 | 115.7 | 5.6 |
| 1040 | 24.26 | 0.07 | 0.025 | 0.003 | 0.055 | 0.007 | 0.017 | 0.003 | 50.2 | 120.2 | 5.0 |
| 1130 | 23.26 | 0.01 | 0.016 | 0.001 | 0.009 | 0.003 | 0.0084 | 0.0005 | 86.4 | 129.1 | 1.4 |
| 1180 | 25.6 | 0.1 | 0.013 | 0.004 | 0.02 | 0.01 | 0.016 | 0.005 | 100.0 | 129.6 | 9.4 |

Note. J, Parameter characterizing the magnetude of the neutron flux.

released, and the last stage with the highest temperature for 45%. Given the specific features of amphibole degassing in $^{40}Ar/^{39}Ar$ experiments using gradual heating, it may be assumed that the factual mineral formation age falls within the range starting at 128 Ma.

A $^{40}Ar/^{39}Ar$ age spectrum consisting of six stages (Fig. 7) was obtained based on ground mass from a monzonite-porphyry dike (sample IN15-11, Fig. 2, Table 1). Three medium-temperature stages may be combined into the age plateau. The average weighted age of the obtained age plateau is 130 ± 2.4 Ma. The volume of $^{39}Ar$ released within the age plateau reaches 70% (Table 1). The age obtained corresponds to the closure age of the $^{40}Ar/^{39}Ar$ isotopic system in the ground mass of the porphyry sample and fits with the monzonite porphyry formation time.

The age spectrum obtained as a result of $^{40}Ar/^{39}Ar$ dating of phlogopite from shonkinites (sample 2224, Fig. 2) consists of eight stages (Fig. 7). The nature of the spectrum does not make it possible to conclusively identify the age plateau, and the sample formation age is estimated based on two high-temperature stages at 129 ± 1.4 Ma. The amount of the gas released within the last two stages is 50%.

## DISCUSSION

The $^{40}Ar/^{39}Ar$ dating results obtained make it possible to confine the formation time of the main volume of alkaline rocks to 133–128 Ma. With the analytical error taken into account, it may be assumed that the shonkinites, leuco- and melanocratic syenites, and monzonite porphyry of the Inagli massif were formed almost simultaneously. The age of veins intrusion into the core is clearly identified at 133.4 ± 1 Ma based on amphibole from the pegmatite amphibole-feldspar vein with Cr-diopside phenocrysts. Geological observations show similar veins overlapping both dunites and clinopyroxenite dikes in the core, thereby marking 133.4 ± 1 Ma as the upper age estimate for these rocks. Pegmatite vein formation is directly associated with the intrusion of the alkaline rock mass with accompanying autometasomatism.

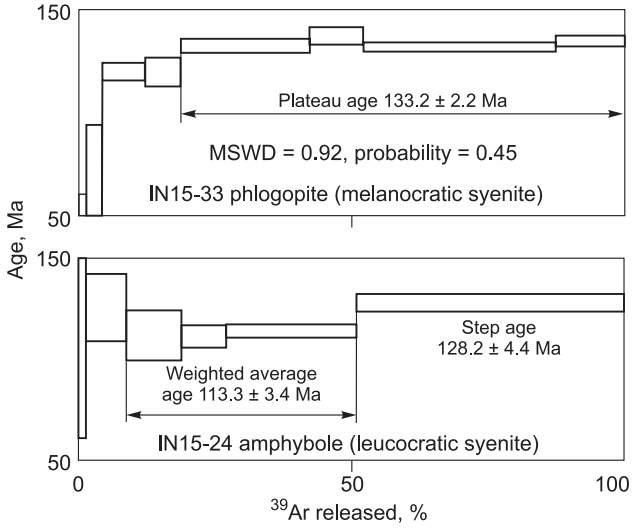


**Fig. 6.** $^{40}Ar/^{39}Ar$ dating results for monomineral phlogopite fractions from melanocratic syenites (sample IN15-33) and amphibole from leucocratic syenites (sample IN15-24). The error is presented with ±2σ interval.

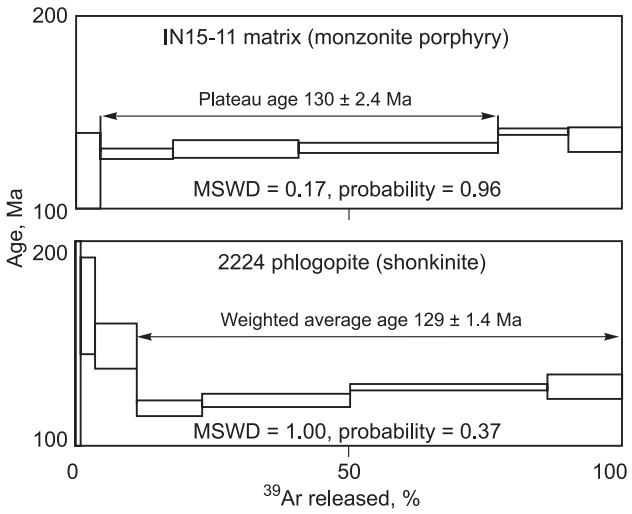


**Fig. 7.** $^{40}Ar/^{39}Ar$ dating results for the ground mass of monzonite-porphyry (sample IN15-11) and phlogopite from shonkinites (sample 2224) in the Inagli massif. The error is presented with ±2σ interval.

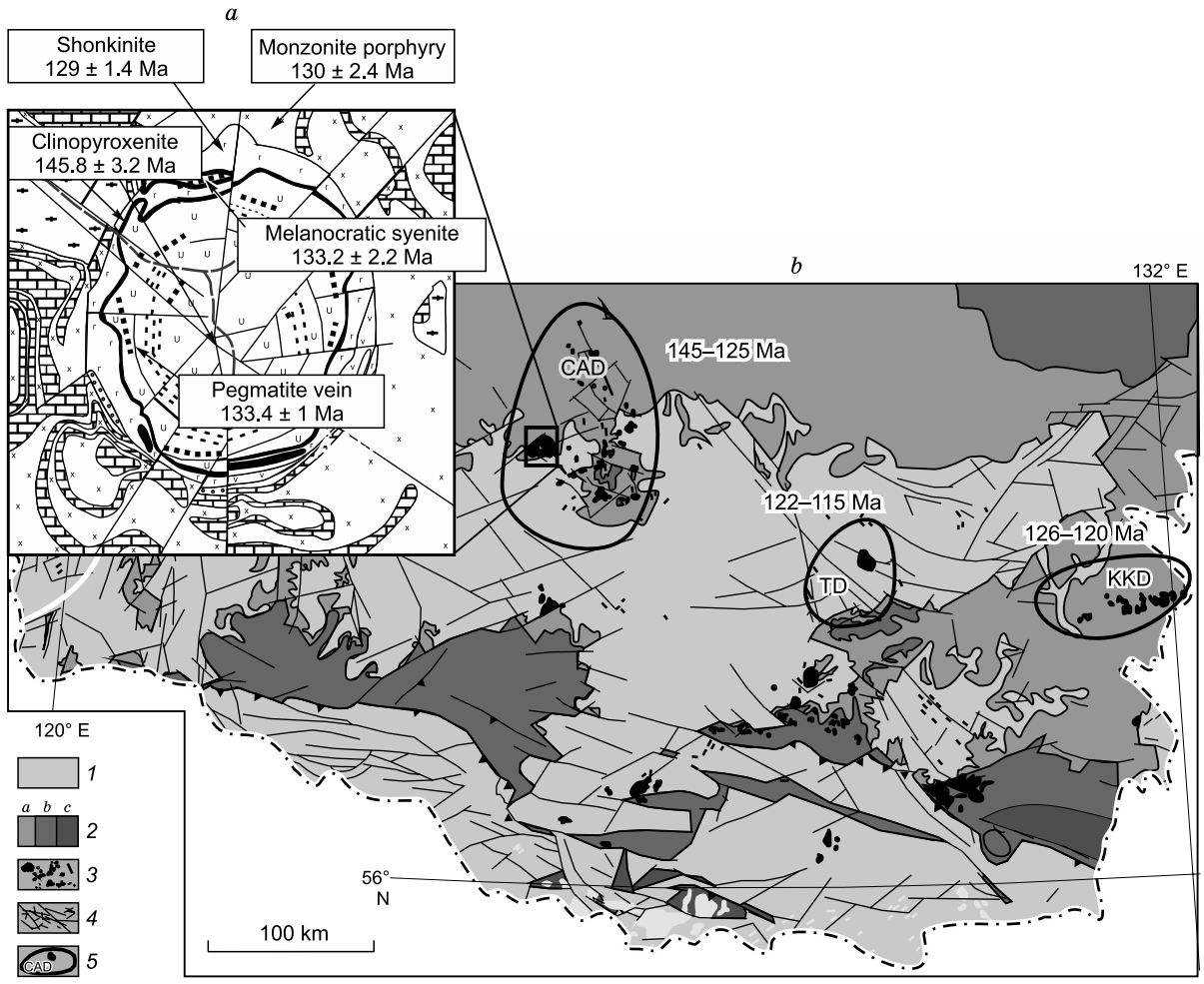


**Fig. 8.** Scheme of the Inagli massif (*a*) with the layout of ore districts within the Chara–Aldan metallogenic zone of the Aldan–Stanovoi Shield (*b*) with geochronological data (geological plot based on (Dzevanovskii et al., 1972), ore districts are shown based on (Parfenov and Kuz'min, 2001)). *1*, shield base; *2*, cover rocks: I, Proterozoic sandstones and Cambrian limestones, II, Jurassic sandstones, III, Cretaceous sandstones; *3*, Mesozoic igneous rocks; *4*, faults; *5*, outlines of ore districts associated with Mesozoic alkaline magmatism: CAD, Central Aldan district; TD, Tyrkanda district; KKD, Ket-Kap district. Geochronological data are obtained using U–Pb and Ar–Ar methods (Borisenko et al., 2011; Polin et al., 2012; Prokopyev et al., 2018).

Clinopyroxenite formation appears isolated at the age 145.8 ± 3.2 Ma at most. These rocks form a thin outer zone around the core, the dikes with a similar composition being observed within the core as well (Boyarko and Prokopchuk, 2002). It is possible that clinopyroxenite intrusion was the earliest event of the ring formation, which followed formation of the older dunite core. However, simultaneous formation (or transformation) of dunites and clinopyroxenites still remains a possibility. A significant error in determination of the age of phlogopite impregnation in dunites (136.5 ± 5.3 Ma) complicates the conclusive interpretation, i.e., with the error taken into account, the result overlaps with both phlogopite clinopyroxenite formation time and the age of amphibole-feldspar veins. In addition, the dating obtained based on phlogopite from dunites overlaps with the age of zircons from dunites of the massif (U–Pb SHRIMP II method), i.e., 134 ± 2 Ma (Ibragimova et al., 2015), which makes it possible to assume the possibility of co-formation or recrystallization of zircon and phlogopite.

Age values determined for the Inagli massif rocks match in time with late Mesozoic magmatic processes widely represented in the Aldan Shield. Aldan late Mesozoic magmatic complexes typically have linear-cluster placement of magmatic bodies with changes in rock composition in both S–N and E–W directions. In particular, rocks in the western part of the shield have high alkalinity, subalkaline rocks being relatively rare, whereas subalkaline rocks and granites are more common for the eastern margin. Multiple attempts have been made to use formation analysis to obtain an integral view of the Mesozoic magmatism of the Aldan Shield with its extreme variety of igneous rock composition (Mironyuk, 1971). Both geological data and K–Ar dating for the Central Aldan ore district were used to define the following formation stages of rock associations:

(1) Early Jurassic monzonite-syenite at 217–186 Ma;

(2) Middle Jurassic dunite and leucitite-alkaline syenite at 175–161 Ma;

(3) Late Jurassic–Early Cretaceous fergusite-dunite and monzonite-syenite at 162–140 Ma;

(4) Early Cretaceous leucitite-alkaline syenite, monzonite-syenite and leucitite-alkaline syenite at 138–125 Ma (Maksimov et al., 2010).

A flaw should be noted in this classification, as it relies on obsolete K–Ar dating results significantly inferior to the presently available precise age determination methods. In particular, it was assumed earlier that the Inagli massif formation occurred in two stages: (1) dunite core, pyroxenite, and melashonkinite formation in the Early Jurassic; (2) fergusonite, missourite, pseudoleucite shonkinite, and syenite formation in the Late Jurassic (Maksimov, 1975; Maksimov et al., 2010). The authors of the present paper showed that the formation of clinopyroxenites (145.8 ± 3.2 Ma) and alkaline-basic rocks (133–128 Ma) occurred in the Cretaceous.

The Ryabinovy syenite massif in the Central Aldan (gold ore) district is considered a reference structure, where all Mesozoic alkaline magmatism stages, namely $T_3$–$J_1$, $J_1$–$J_2$, $J_3$–$K_1$, and $K_1$–$K_2$ are manifested (Kochetkov et al., 1989; Maksimov, 2003). The age of sericite-microcline metasomatites within the Ryabinovyi massif based on K–Ar dating results is 134–120 Ma (Ugryumov and Dvornik, 1985; Dvornik, 2009). Ar–Ar dating results for orthoclase from alkaline syenite of the massif showed the rock formation age of 144.8 ± 1.5 Ma (Borisenko et al., 2011), which matches with the clinopyroxenite age (145.8 ± 3.2 Ma) in the Inagli massif obtained in the present paper. Later lamprophyre dikes of the Ryabinovyi massif were dated at 129–125 Ma (Borisenko et al., 2011), which is also close to the age of alkaline syenite complex in the Inagli massif (133–128 Ma). The latest papers by (Shatov et al., 2012) showed an almost identical (Early Cretaceous–Late Jurassic) age of syenite and lamprophyre crystallization in the Ryabinovyi massif of 147–120 Ma based on independent U–Pb and Rb–Sr isotopic systems. Lamprophyres within the Lebedinoe ore field (Central Aldan ore district) have a close age of 132.4 ± 1.6 Ma ($^{40}Ar/^{39}Ar$ dating of phlogopite, (Borisenko et al., 2011)). According to the $^{40}Ar/^{39}Ar$ dating of phlogopite from syenites of the Lunnoe deposit (southwestern part of the Elkon horst), the rock formation age of 143.1 ± 2.0 Ma is obtained (authors' data).

The evolution of Mesozoic alkaline ore-magmatic systems of the Central Aldan district falls into the interval of about 145–120 Ma. In addition, key ore-production stages in the Ryabinovoe, Kuranakh, and Lebedinoe deposits fall into a rather narrow range at about 137 Ma, which implies their simultaneous formation in different areas of the Central Aldan alkaline complex (Borisenko et al., 2011). U–Pb dating results for the Elkon gold-uranium ore-magmatic system showed that magmatic and hydrothermal-metasomatic activity within the ore cluster falls into the range of 143–125 Ma (Kazanskii, 2004; Terekhov, 2012). The age interval obtained for the Inagli massif formation (142–128 Ma) matches the general geochronology of the Central Aldan district.

The Murun Mesozoic alkaline complex consisting of the Bolshoi Murun massif and the Dolgadyn alkaline syenite intrusion of the Malyi Murun massif is located in the northwest of Aldan Shield. Ar/Ar dating results for feldspar and tinaksite of the Malyi Murun massif are 134.1 ± 2.9 and 133.0 ± 3.0 Ma, respectively. This age matches with the formation of the charoite deposit and the metasomatic area of the massif (Wang et al., 2014). Charoite formation dating results obtained based on tinaksite, tokoite, microcline, and frankamenite monofractions using adjusted $^{40}K$ decay constants are 135.9 ± 0.49, 135.87 ± 0.45, 135.79 ± 0.42, and 137.55 ± 0.46 Ma, respectively (Ivanov et al., 2018). The use of adjusted constants, as opposed to the conventional ones, provides a slight increase of about 1% in the ages obtained compared to the earlier publications (Wang et al., 2014).

The Tyrkanda gold ore district is identified to the southeast of the Central Aldan ore district (at approximately 200 km) (Vetluzhskikh, 1990). According to the Rb–Sr and Ar–Ar dating results, the age of alkaline rocks in the Dzheltula syenite massif of the Tyrkanda district falls into the interval of 138–115 Ma (Kravchenko et al., 2014; Prokopyev et al., 2018), while formation ages of main alkaline phases and the dike complex fall into a rather narrow interval of 121–118 Ma (Ar–Ar method, (Prokopyev et al., 2018)). The Ket-Kap ore district is located to the east of the Tyrkanda district (at approximately 150–200 km). The latest U–Pb isotopic dating results for zircons and titanates in subalkaline magmatism outcrops in the Ket-Kap–Yuna ore-magmatic system showed that Mesozoic magmatism continued for only a few million years and was confined to the Early Cretaceous stage of 126–120 Ma (Polin et al., 2012).

Thus, the projected age zone distribution of alkaline Mesozoic magmatism is confirmed (Prokopyev et al., 2018), i.e., alkaline rock rejuvenation from Central Aldan towards eastern districts of the Aldan Shield. In addition, simultaneous magmatism manifestations in the western part of the Aldan Shield (Murun alkaline complex) and in the Central Aldan district are observed.

## CONCLUSIONS

The Inagli alkaline-ultrabasic massif is a unique structure in the Central Aldan ore district, where multistage Mesozoic alkaline magmatism and its accompanying mineralization (vein crystallization with Cr-diopside and vermiculite) are manifested. According to the Ar–Ar dating results, it was found that the intrusion of alkaline rocks of the massif occurred at least in two stages: (1) crystallization of the dunite core rim represented by clinopyroxenites dated at 145.8 ± 3.2 Ma at most; and (2) formation of a differentiated alkaline

ring of the massif in the interval of 133–128 Ma: crystallization age for melanocratic syenites is 133.2 ± 2.2 Ma, for monzonite porphyry 130 ± 2.4 Ma, for leucocratic syenites 128.2 ± 4.4 Ma at most, and for shonkinites 129 ± 1.4 Ma at most. The formation age of phlogopite impregnation in dunites is 136.5 ± 5.3 Ma (based on phlogopite dating), while the formation age of ore veins (based on amphibole from the feldspar-chrome diopside-mica vein) is 133.4 ± 1 Ma.

**Acknowledgments.** The Ar–Ar isotopic geochronological study of alkaline rocks of the Inagli massif was supported by the Russian Foundation for Basic Research, project No. 16-35-00335. The petrographic investigation of the massif's rocks was performed under the Russian Scientific Foundation grant (project No. 15-17-20036). The work was performed within the framework of the state assignment, projects Nos. 0330-2016-0013 and 0330-2016-0002.

## REFERENCES

Bilibin, Yu.A., 1958. Selected Works. Vol. 1 [in Russian]. Akad. Nauk SSSR, Moscow.

Borisenko, A.S., Gas'kov, I.N., Dashkevich, E.G., Okrugin, A.M., Ponomarchuk, A.V., Travin, A.V., 2011. Geochronology of magmatic processes and ore formation in the Central Aldan gold-ore region, in: Int. Symp. Large Igneous Provinces of Asia. Irkutsk, pp. 38–39.

Boyarko, G.Yu., Prokopchuk, S.I., 2002. Geochemical exploration for platinum (Inagli intrusion, Aldan Shield), in: Applied Geochemistry. Vol. 3: Prediction and Prospecting [in Russian]. IMGRE, Moscow, pp. 562–569.

Campbell, I.H., Naldrett, I.H., Barnes, S.J., 1983. A model for the origin of platinum-rich sulfide horizons in the Bushveld and Stillwater Complexes. J. Petrol. 24 (2), 133–165.

Cawthorn, R.G., Merkle, R.K., Vilojen, M.J., 2002. Platinum-group elements deposits in the Bushveld complex, South Africa, in: Cabri, L.J. (Ed.), The Geology, Geochemistry, Mineralogy, and Mineral Beneficiation of Platinum-Group Elements. Canadian Institute of Mining and Metallurgy, Ottawa, Ontario. Spec. Vol. 54, pp. 389−429.

Dvornik, G.P., 2009. Sericite-microcline metasomatites and gold mineralization of the Ryabinovyi ore field (Aldan Shield). Litosfera, No. 2, 56–66.

Dzevanovskii, Yu.K., Vorona, I.D., Lagzdina, G.Yu., 1972. Geological Map of the Southern Part of Yakutian ASSR [in Russian]. Leningradskaya Kartfabrika VAGT, Leningrad.

El'yanov, A.A., Moralev, V.M., 1961. New data on age of ultrabasic and alkaline rocks of the Aldan Shield. Dokl. Akad. Nauk SSSR 141 (3), 687–689.

Fleck, R.J., Sutter, J.F., Elliot, D.H., 1977. Interpretation of discordant $^{40}Ar/^{39}Ar$ age-spectra of Mesozoic tholeiites from Antarctica. Geochim. Cosmochim. Acta 41 (1), 15–32.

Genkin, A.D., 1997. Sequence and formation conditions of platinum group minerals in Nizhnii Tagil massif. Geologiya Rudnykh Mestorozhdenii 39 (1), 41–48.

Glagolev, A.A., Korchagin, A.M., Kharchenkov, A.G., 1974. Arbarastakh and Inagli Alkaline-Ultrabasic Massifs [in Russian]. Nauka, Moscow.

Gurovich, V.G., Emel'yznenko, E.P., Zemlyanukhin, V.N., Karetnikov, A.S., Kvasov, A.I., Lazarenkov, V.G., Malitch, K.N., Mochalov, A.G., Prikhod'ko, V.S., Stepashko, A.A., 1994. Geology, Petrology, and, Mineralization of the Konder Massif [in Russian]. Nauka, Moscow.

Ibragimova, E.K., Radkov, A.V., Molchanov, A.V., Shatov, V.V., Lepechina, E.N., Antonov, A.V., Tolmacheva E.V., Soloviev, O.L., Terekhov, A.V., Horohorina, E.I., 2015. The results of U–Pb (SHRIMP II) isotope dating of zircons from dunite from massif Inagli (Aldan Shield) and the problem of the genesis of concentrically-zoned complexes. Regional'naya Geologiya i Metallogeniya 62, 64–78.

Ivanov, A.V., Gorovoy, V.A., Gladkochub, D.P., Shevelev, A.S., Vladykin, N.V., 2018. The first precise data on the age of charoite mineralization (Eastern Siberia, Russia). Dokl. Earth Sci. 478 (2), 179–182.

Karetnikov, A.S., 2009. Paleomagnetism of ultramafics of the Konder massif and its age assessment. Russ. J. Pacific Geol. 3: 530. DOI:10.1134/S1819714009060025.

Kazanskii, V.I., 2004. The unique Central Aldan gold-uranium ore district (Russia). Geologiya Rudnykh Mestorozhdenii 46 (3), 195–211.

Kochetkov, A.Ya., 1984. PGE-type geochemical specialization of ore-bearing alkaline complexes of Central Aldan, in: Bull. NTI. Geology and Mineral Resources of Yakutia [in Russian]. YaF SO AN SSSR, Yakutsk, pp. 25–27.

Kochetkov, A.Ya., Pakhomov, V.N., Popov, A.B., 1989. Magmatism and metasomatism of the Ryabinovy alkaline ore-bearing massif (Central Aldan), in: Magmatism of Copper-Molybdenum Ore Clusters [in Russian]. Nauka, Novosibirsk, pp. 79–110.

Kochetkov, A.Ya., 2006. Mesozoic gold-bearing ore-magmatic systems of Central Aldan. Russian Geology and Geophysics (Geologiya i Geofizika) 47 (7), 847–861 (850–864).

Korchagin, A.M., 1966. Inagli vermiculite-phlogopite deposit. Izvestiya Akad. Nauk SSSR. Ser. Geol. No. 8, 15–27.

Kostyuk, V.P., Panina, L.I., Zhidkov, A.Ya., Orlova, M.P., Bazarova, T. Yu., 1990. K-Alkaline Magmatism of Baikal–Stanovoi Riftogenic System [in Russian]. Nauka, Novosibirsk.

Kravchenko, A.A., Ivanov, A.I., Prokop'ev, I.R., Zaitsev, A.I., Bikbaeva, E.E., 2014. Features of composition and formation age of mesozoic intrusions of Tyrkanda ore region of Aldan-Stanovoi Shield. Otechestvennaya Geologiya, No. 5, 43–52.

Maksimov, E.P., 1975. An attempt at formation analysis of Mesozoic magmatic structures of the Aldan Shield. Izvestiya Akad. Nauk SSSR. Ser. Geol., No. 4, 16–32.

Maksimov, E.P., 2003. Mesozoic Ore-Bearing Magmatogenic Systems of the Aldan-Stanovoi Shield. ScD Thesis [in Russian]. Yakutsk.

Maksimov, E.P., Uyutov, V.I., Nikitin, V.M., 2010. The Central Aldan gold-uranium ore magmatogenic system (Aldan-Stanovoi Shield, Russia). Russ. J. Pacific Geol. 4 (2), 95–115.

Malitch, K.N., 1999. Platinum-Group Elements in Clinopyroxenite-Dunite Massifs of the East Siberia (Geochemistry, Mineralogy, and Genesis) [in Russian]. VSEGEI, St. Petersburg.

Malitch, K.N., Efimov, A.A., Badanina, I.Yu., 2012. The age of Kondyor massif dunites (Aldan Province, Russia): First U–Pb isotopic data. Dokl. Earth Sci. 446 (1), 1054–1058.

Mironyuk, E.P., 1971. Geology of western part of the Aldan Shield [in Russian]. Nedra, Moscow.

Mues-Schumacher, U., Keller, J., Kononova, V.A., Suddaby, P.J., 1996. Mineral chemistry and geochronology of the potassic alkaline ultramafic Inagli complex, Aldan Shield, eastern Siberia. Mineral. Mag. 60 (402), 711–730.

Okrugin, A.V., 2004. Crystallization-liquation model of the formation of PGE-chromitite ores in mafic-ultramafic complexes. Tikhookeanskaya Geologiya 23 (2), 63–65.

Parfenov, L.M., Kuz'min, M.I., 2001. Tectonics, Geodynamics, and Metallogeny of the Sakha Republic (Yakutia) [in Russian]. MAIK Nauka/Interperiodica, Moscow.

Polin, V.F., Mitsuk, V.V., Khanchuk, A.I., Glebovitskii, V.A., Budnitskii, S.Yu., Rizvanova, N.G., Solyanik, A.N., Shishov, A.S., 2012. Geochronological limits of subalkaline magmatism in the Ket-Kap–Yuna igneous province, Aldan Shield. Dokl. Earth Sci. 442 (1), 17–23.

Prokopyev, I.R., Kravchenko, A.A., Ivanov, A.I., Borisenko, A.S., Ponomarchuk, A.V., Zaitsev, A.I., Kardash, E.A., Rozhkov, A.A., 2018. Geochronology and ore mineralization of the Dheltula alka-

line massif (Aldan Shield, South Yakutia). Russ. J. Pacific Geol. 12 (1), 34–45.

Pushkarev, Yu.D., Kostoyanov, A.I., Orlova, M.P., Bogomolov, E.S., 2002. Special features of Rb–Sr, Pb–Pb, Re–Os, and K–Ar isotopic systems in the Konder massif: PGE-enriched mantle substrate. Regional'naya Geologiya i Metallogeniya, No. 16, 80–91.

Ronkin, Yu.L., Efimov, A.A., Lepikhina, G.A., Rodionov, N.V., Maslov, A.V., 2013. U–Pb dating of the baddeleytte-zircon system from Pt-bearing dunite of the Konder massif, Aldan Shield: New data. Dokl. Earth Sci. 450 (2), 607–612.

Rozhkov, I.S., Kitsul, V.I., Razin, L.V., Borishanskaya, S.S., 1962. Platinum of the Aldan Shield [in Russian]. Akad. Nauk SSSR, Moscow.

Shatov, V.V., Molchanov, A.V., Shatova, N.V., Sergeev, S.A., Belova, V.N., Terekhov, A.V., Rad'kov, A.V., Soloviev, O.L., 2012. Petrography, geochemistry and isotopic (U–Pb and Rb–Sr) dating of alkaline ugneous rocks of the Ryabinovyi stock (Southern Yakutia). Regional'naya Geologiya i Metallogeniya 51, 62–78.

Shnai, G.K., 1980. Dunite heterogeneity in ultrabasic-alkaline massifs (the example of Inagli massif). Izvestiya Akad. Nauk SSSR. Ser. Geol., No. 4, 23–35.

Shukolyukov, Yu.A., Yakubovich, O.V., Mochalov, G.K., Kotov, A.B., Sal'nikova, E.B., Yakovleva, S.Z., Korneev, S.I., Gorokhovskii, B.M., 2012. New geochronometer for the direct isotopic dating of native platinum minerals ($^{190}$Pt–$^{4}$He method). Petrology 20 (6), 545–599.

Terekhov, A.V., 2012. Ore-Bearing Capacity of Hydrothermal-Metasomatic Structures of Elkon Gold-Uranium Cluster. PhD Thesis [in Russian]. Yakutsk.

Travin, A.V., 2016. Thermochronology of Subduction-Collision and Collision Events in Central Asia. PhD Thesis [in Russian]. Novosibirsk.

Steiger, R.H, Jäger, E., 1977. Subcommission on Geochronology: Convention on the use of decay constants in geo- and cosmochronology. Earth Planet. Sci. Lett. 36 (3), 359–362.

Ugryumov, A.N., Dvornik, G.P., 1985. Sericite-microcline metasomatites from the Ryabinovyi massiv (Central Aldan). Dokl. AN SSSR 280(1), 191—193.

Ugryumov, A.N., Kiselev, Yu.V., 1969. The age of ultrabasic rocks of the Inagli massif (Aldan Shield). Geologiya i Geofizika, No. 8, 19–24.

Vetluzhskikh, V.G., 1990. Gold Mineralization at the Age of Mesozoic Tectonomagmatic Activity of the Aldan-Stanovoi Province. ScD Thesis [in Russian]. Moscow–Yakutsk.

Vetluzhskikh, V.G., Kazanskii, V.I., Kochetkov, A.Ya., Yanovskii, V.M., 2002. Central Aldan gold deposits. Geologiya Rudnykh Mestorozhdenii 44 (6), 467–499.

Wang, Y., He, H., Ivanov, A.V., Zhu, R., Lo, C., 2014. Age and origin of charoitite, Malyy Murun massif, Siberia, Russia. Int. Geol. Rev. 56 (8), 1007–1019.

*Editorial responsibility:* E.V. Sklyarov